# Combining MISR, ETM+ and SAR data to improve land cover and land use classification for carbon cycle research

Xue Liu  Menas Kafatos  Richard B. Gomez

Center for Earth Observing and Space Research
School of Computational Sciences, George Mason University, Fairfax, VA 22030-4444

Scott J. Goetz

Geography Department, University of Maryland, College Park, MD 20742-8225
& Woods Hole Research Center, Woods Hole, MA 02543-0296

*Abstract* — **Accurate and reliable information about land cover and land use is essential to carbon cycle and climate change modeling. While historical regional-to-global scale land cover and land use data products had been produced by AVHRR and MSS/TM, this task has been advanced by sensors such as MODIS and ETM since the latter 1990s. While the accuracies and reliabilities of these data products have been improved, there have been reports from the modeling community that additional work is needed to reduce errors so that the uncertainties associated with the global carbon cycle and climate change modeling can be addressed. Remotely sensed data collected in different wavelength regions, at different viewing geometries, usually provide complementary information. Their combination has the potential to enhance remote sensing capabilities in discriminating important land cover components. In this paper, we studied multi-angle data fusion, and optical - SAR data fusion for land cover classification at regional spatial scale in the temperate forests of the eastern United States. Data from EOS-MISR, Landsat-ETM+ and RadarSat-SAR were used. The results showed significantly improved land cover classification accuracy when using the data fusion approach. These results may benefit future land cover products for global change research.**

*Keywords*—**Remote sensing, Data fusion, Land cover and land use, Classification, Temperate forest, Carbon cycle, Global change**

## I. INTRODUCTION

According to the most recent IPCC report, about 20-25% of the current increase in atmospheric $CO_2$ of 3.2 gigatones (GT) per year is contributed by changes in land cover and land use [1]. The uncertainty related to this estimation remains as large as ± 30%, with the greatest uncertainty associated with error in rates of land-use change [2].

There is a consensus in the global change research community that satellite remote sensing is the best feasible way to reduce uncertainties at regional-to-global scales [1] [3]-[7]. Commonly used remote sensing data for land cover and land use mapping include AVHRR, MSS/TM, JERS-1, etc. The low spectral resolution provided by these instruments, however, reduces the likelihood of achieving high local classification accuracy [1].

Different materials have different spectral characteristics in different wavelength regions at different viewing geometries. Therefore, data from various sensors collected in different manners may provide complementary spectral information. Fusing the information from different sensors collected in different manners has the potential to enhance remote sensing capabilities of discriminating among materials.

This paper reports on progress made in multi-angle data fusion, as well as optical data and SAR data fusion, for land cover and land use classification in the temperate forest of the eastern United States. Two cases were studied: coarse and moderate spatial resolution. For the coarse resolution (1-km), classifications made using both nadir and multiple view angle data, were compared using MISR data. For the medium spatial resolution (30m) case, classifications made by different combinations of visible, near infrared (NIR), shortwave infrared (SWIR) and synthetic aperture radar (SAR) were compared using ETM+ data and RadarSat data.

## II. ACCURACY CRITERIA

Although it is difficult to quantitatively specify the accuracy criteria for carbon cycle and climate change modeling based on land cover and land use classifications, there is much evidence in the literature that errors in the input land cover and land use parameters - particularly the rates of land use change - need to be decreased if emissions of carbon are to be determined with high precision [1]. For example, errors associated with the rates of land use change estimated from remote sensing data vary greatly. In the tropical Amazon

region, the highest estimate of tropical deforestation ($8.0 \times 10^6$ ha/yr) is 5 times higher than the lowest estimate ($1.5 \times 10^6$ ha/yr) [8] [9]. The classification accuracy of land cover types affects the accuracy of parameters derived from them, such as area extent, change rate, and the other area related parameters. We equate the accuracy (percent correct) of land cover and land use classification as a baseline for assessment of accuracy improvements in the comparisons that follow.

## III. STUDY SITE AND DATA

We chose two areas in the eastern United States, one located in Virginia and the other in Maryland, as our research sites. The Middle Atlantic region hosts various temperate forest ecosystems, including deciduous and evergreen forest, and other land cover and land use types such as croplands, grasslands, shrub-lands, wetlands, etc.

We collected MISR data from NASA-Langley DAAC through the EOS-Gateway. The MISR data are the Level 1B terrain-corrected radiances containing all the nine viewing angles. We also collected Landsat ETM+ data and RadarSat C-band HH polarization data.

During the summer of 2003, a field trip was conducted in Virginia and Maryland to collect field validation information for this research. Sites were georeferenced with a portable GPS receiver. Over 100 sampling points with various land cover and land use type information have been collected.

## IV. DATA PREPROCESSING

One of the important aspects in remote sensing data fusion is to make sure that all the data sets to be fused have the same geographic reference accuracy and are calibrated to the same reference atmospheric conditions.

The preprocessing of MISR level 1B data included co-registration of different view images, and calculation of TOA BRF (Top of Atmosphere Bidirectional Reflectance) for each individual view and each band and mosaic of image blocks. The preprocessing of Landsat ETM+ and Radarsat C-band SAR data included the range-to-ground transformation, adaptive filtering to remove the speckles, re-sampling of SAR image to uniform its spatial resolution, co-registration of SAR data with ETM+ data, etc.

For the ETM+ and SAR data fusion, since our study area is relatively small and terrain in the region is relatively flat, we assume the same atmospheric and terrain effects across each individual scene.

## V. MISR - NADIR VERSUS MULTI-ANGULAR CLASSIFICATION

MISR has nine view angles imaging the Earth simultaneously at angles 26.1°, 45.6°, 60.0° and 70.5°, both forward and afterward of the local vertical, in addition to the nadir view. Each view angle includes four spectral bands – Blue (0.446μm), Green (0.558μm), Red (0.672μm) and Near Infrared (0.867μm) [10][11].

When comparing the differences between nadir-based and multi-angle-based classification, we applied the same classification procedure - K-means unsupervised classification constrained by a maximum of eight clusters. For the nadir view classification, the spectral feature space is four dimensional, thus the spectral feature for each pixel can be expressed as

$$S = (B, G, R, NIR) \quad (1)$$

For the multiple angle view classification, we added four view angles including two forwards and two aft of view angle 26.1° and view angle 45.6°, thus the spectral feature space is twenty dimensional and the spectral feature for each pixel can be expressed as

$$S = (S_1, S_2, S_3, S_4, S_5) \quad (2)$$

where $S_i$ indicates the four-dimensional spectral feature space at each angle from BF to BA views. We did not use the other two forwards and two aft views, since their viewing angles are so large that the number of pixels blocked by angular view is too high. The original MISR images are shown in Fig. 1 and image spectral curves from each of them are shown in Fig. 2.

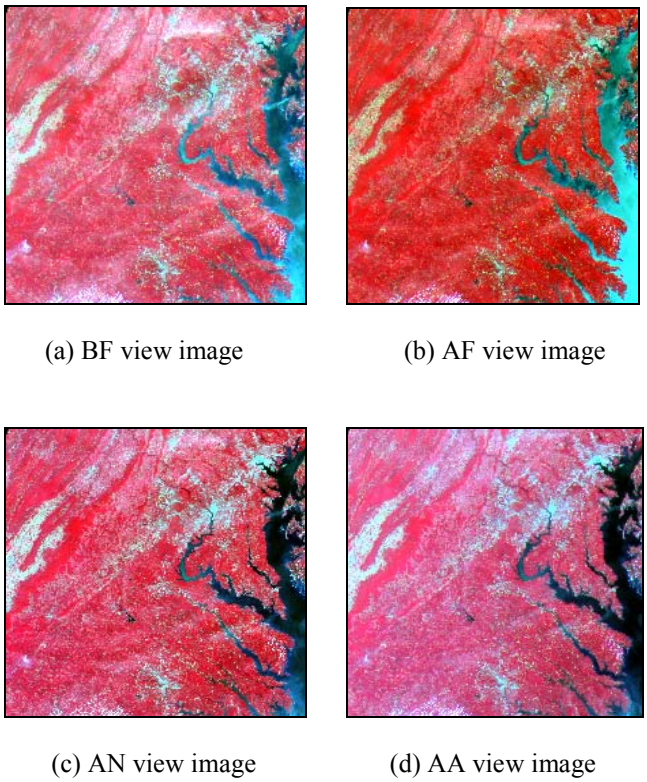

(a) BF view image (b) AF view image

(c) AN view image (d) AA view image

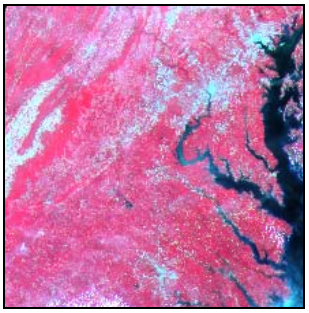

(e) BA view image

**Fig. 1** Illustration of the original MISR images at the five view angles, show as false-color composites of the NIR, Red and Green bands.

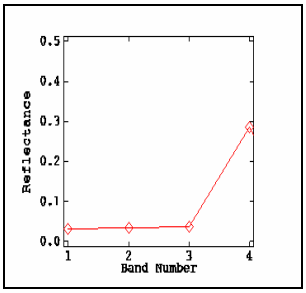


(a) BF view

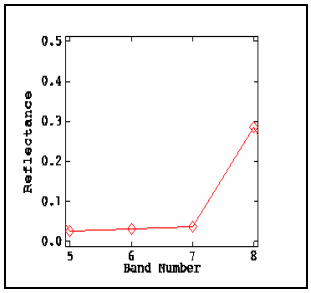


(b) AF view

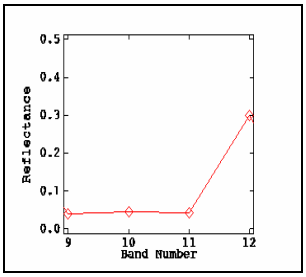


(c) AN view

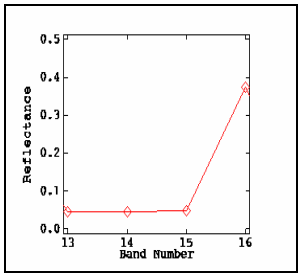


(d) AA view

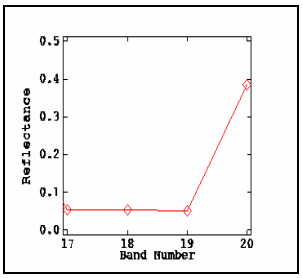


(e) BA view

**Fig. 2** Illustration of image spectral curves at the five view angles, showing the TOA-BRF.

We focused on only the major land cover types, particularly vegetated classes. We took *Deciduous Forest* as an example in the classification to examine the improvement in classification accuracy, since we have more field validation than for other land cover and land use types.
The classification results are shown in Fig. 3 and Fig. 4.

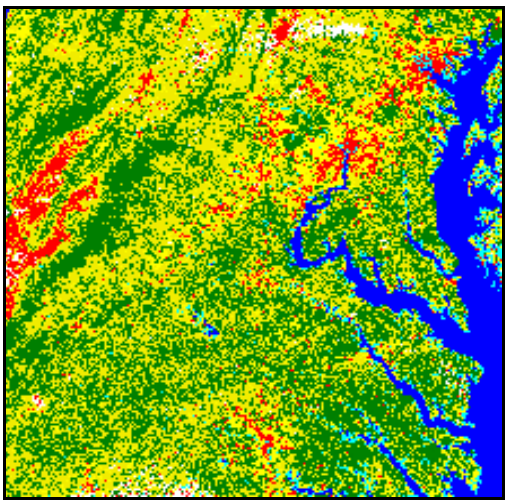

(a)

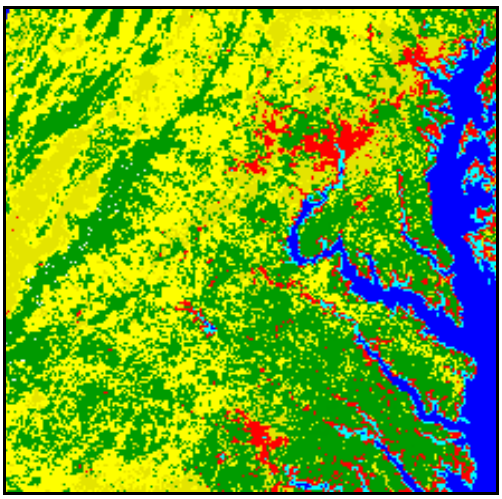

(b)

**Fig. 3** Classification based on MISR nadir view versus five angle views. The dark green color on all the images indicates *Deciduous Forest*. (a) Classification based on nadir view only using K-means unsupervised classification and classes were labeled by referencing the ground truth information and TM-based classification when necessary.

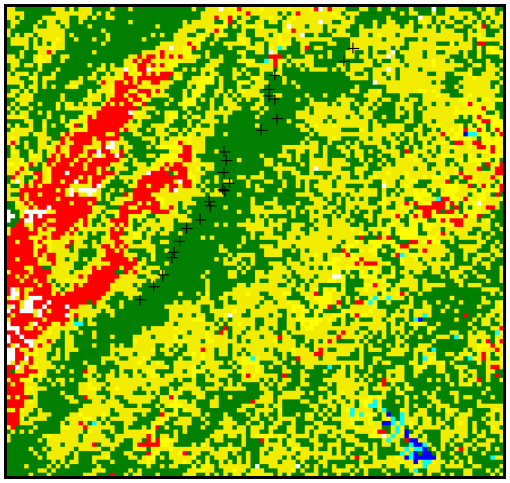

(a)

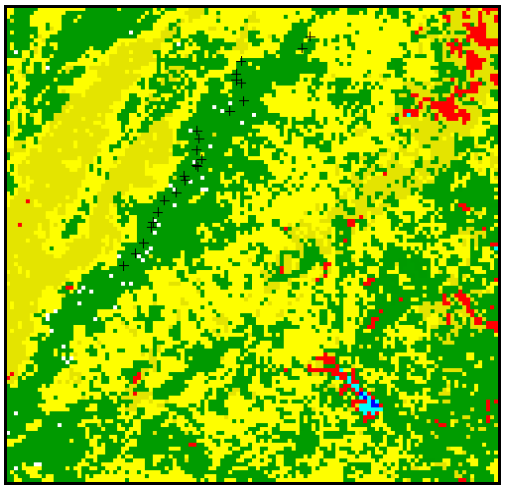

(b)

**Fig. 4** Expanded view of the images in Fig. 3 showing the field validation points (black pluses) for *Deciduous Forest*. (a) Classification based on nadir view only; (b) Classification based on five angular views.

Based on comparison between the two classifications and referencing the field information collected in the Shenandoah National Park (n=23) located in Virginia, we note the following:

1) The classification based on five views was much more improved in accuracy than the classification based on nadir view only. For the latter, incorrectly classified pixels accounted for 22% of the total, while for the classification based on five views, incorrectly classified pixels were just 9%.

2) In addition, based on observation and referencing with Shenandoah Park maps, the deciduous forest classification based on multi-angle observation was much improved over the nadir-only classification.

## VI. ETM+ AND SAR - VISIBLE, NIR, SWIR, AND C-BAND HH SAR DATA FUSION

This research site is located at the Patuxent River watershed in Maryland. We used the Visible, NIR and SWIR bands of the eight ETM+ spectral bands: three visible (0.45-0.515μm; 0.525-0.605μm; 0.63-0.690μm), one near infrared (NIR, 0.75-0.90μm), two shortwave infrared bands (SWIR, 1.55-1.75μm and 2.09-2.35μm), one thermal infrared (TIR, 10.40-12.5μm) and one Pan-band (0.52-0.90μm). SAR data were from the Canadian RadarSat sensor, a C-band HH polarization SAR with 5.6cm wavelength. The data were collected in standard mode at 25m resolution. After our preprocessing, the image was re-sampled to 30m resolution to be consistent with the ETM+ data.

We set three different band combination cases for ETM+ and SAR data, and used a *Stacked Vector* data fusion method [12]. After the images were preprocessed and combined, the same unsupervised statistical classification method (K-means) was applied and constrained to eight clusters. We again used *Deciduous Forest* as an example to test the impact on classification accuracy.
The spectral feature space for each case can be expressed as

Case 1: S = (Visible, NIR) (3)
Case 2: S = (Visible, NIR, SWIR) (4)
Case 3: S = (Visible, NIR, SWIR, SAR) (5)

We have 16 sampling points for *Deciduous Forest* in this area (n=16). The classification images for each case are shown in Fig. 5. The classification results are presented in Table 1 and shown in Fig. 6.

TABLE 1
CLASSIFICATION ACCURACIES OF THE *DECIDUOUS FOREST* CLASS USING DIFFERENT DATA COMBINATIONS AND FUSION APPROACHES

| **Fusion case** | **Correct classification (%)** |
|---|---|
| **Case 1:** Visible and NIR | 42% |
| **Case 2:** Visible, NIR and SWIR | 69% |
| **Case 3:** Visible, NIR, SWIR and SAR | 81% |

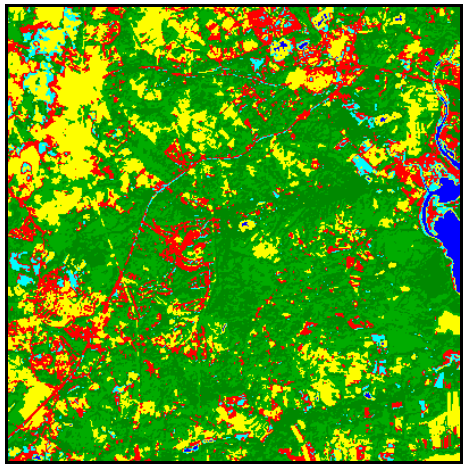

(a)

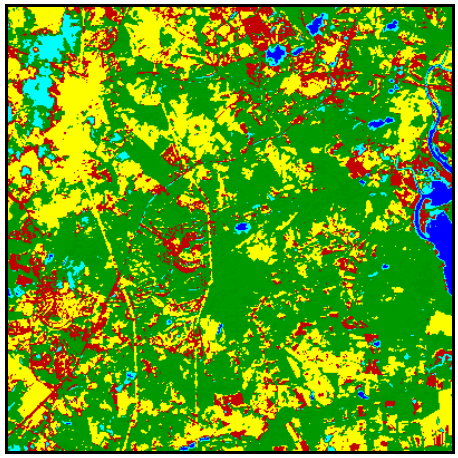

(b)

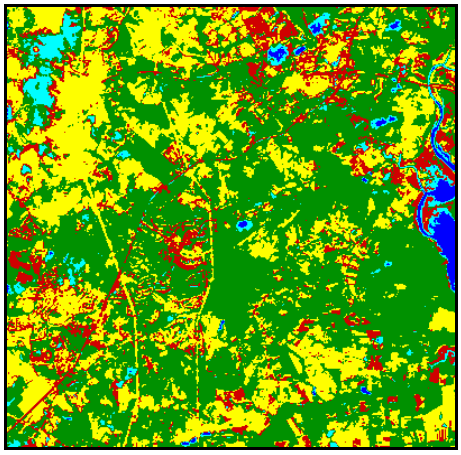

(c)

**Fig. 5** Classification based on different combinations of ETM+ and SAR data. The dark green color on all the images indicates *Deciduous Forest*. (a) Case 1; (b) Case 2; (c) Case 3, each as defined in Table 1.

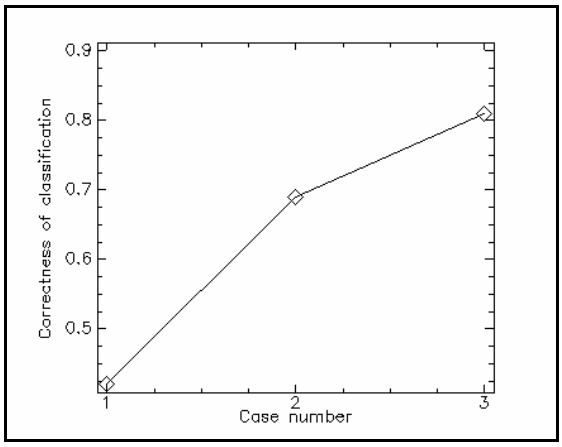


**Fig. 6** Illustration of the improved accuracy in land cover and land use classification by incorporating the SWIR and SAR data. Case 2 incorporated the two SWIR bands and case 3 incorporated the SAR information.

## VII. DISCUSSIONS AND CONCLUSIONS

Generally, the accuracy of land cover classification depends on two factors. One is the amount of the spectral information provided by the input remotely sensed data, the other is the classification approach. For the same set of input remote sensing data, different classification approaches may have quite different accuracies. This is important because land cover and land use data products play an important role in quantitative modeling of carbon cycle and climate change. Input map accuracy is closely related to output uncertainties from these models.

There is evidence that multi-angle observational data are sensitive to vegetation canopy structure or the canopy roughness [13] [14], thus the use of multi-angle data has the potential to increase the accuracy in land cover and land use classification for use in models. Our analysis has demonstrated that accuracy of land cover and land use classifications were substantially improved by fusing multi-angle spectral measurements.

While the information provided by individual remote sensing instrument is not enough to discriminate materials or their parameters with high precision, measurements from different instruments usually have complimentary characteristics [15]. The best way to utilize this information is to combine data from different instruments through data fusion. The three case studies we present using combinations of ETM+ and SAR have demonstrated that the accuracy of land cover and land use classification can be greatly improved by introducing the shortwave infrared data and fusing optical with microwave measurements. We found the highest accuracies can be achieved using a combination of Visible, NIR, SWIR and SAR data.

ACKNOWLEDGEMENTS

This work was supported by the NASA funded project-VAccess / Middle Atlantic Geographic Information Consortium (MAGIC). We thank NASA Langley Atmospheric Sciences Data Center for providing technical support on MISR data, the USGS EROS Data Center for providing the ETM+ data, and a NASA ADRO2 data grant to SJG for the SAR imagery.

REFERENCES

[1] IPCC, (2001) "Climate change 2001 TAR: The scientific basis,"[Online],http://www.grida.no/climate/-ipcc_tar/wg1/096.htm

[2] R. A. Houghton, "Emissions of carbon from land-use change", in *The Carbon Cycle*, edited by T. M. L. Wigley and D. S. Schimel, Cambridge University Press, 2000, pp.63-76

[3] H. J. Shellnhuber, "Earth system analysis and management," in *Understanding the Earth System: Compartments, Processes and Interactions*, edited by E. Ehlers and T. Krafft, Springer, 2001, pp.17-56

[4] G. M. Foody, and P. J. Curran, "Estimation of tropical forest extent and regeneration stage using remotely sensed data," *Journal of Biogeography*, 1994, 21: pp.223-244

[5] R. DeFries, J. Townshend, and M. Hansen, "Continuous fields of vegetation characteristics at the global scale at 1-km resolution," *Journal of Geophysical Research*, 1999, 104(D14), pp.16911-16923

[6] C. Lim and M. Kafatos, "Frequency analysis of natural vegetation distribution using NDVI/AVHRR data from 1981 to 2000 for North America: correlations with SOI," *International Journal of Remote Sensing*, 2002, 23(17): pp.3347-3383

[7] J. Twonshend, C. Justice, W. Li, C. Gurney, and J. McNaus, "Monitoring global land cover: present capabilities and future possibilities." *Remote Sensing of Environment*, 1991, 35:pp.243-256

[8] A. W. Setzer, and M. C. Pereira, "Amazonia biomass burnings in 1987 and an estimate of their tropospheric emissions." Ambio 20, 1991,pp.19-22

[9] D. Skole, and C. Tucker. "Tropical deforestration and habitat fragmentation in the Amazon: Satellite data from 1978 to 1988. " *Science* 260, 1993. pp.1905-1910

[10] D. J. Diner, G. P. Asner, et al., "New directions in Earth Observing: Scientific applications of multiangle remote sensing," *Bulletin of the American Meteorological Society,* 1999, 80(11): pp.2209-2227

[11] NASA, (2003) [Online] http://www-misr.jpl.nasa.gov/

[12] J. A. Richards, and X. Jia, *Remote Sensing Digital Analysis, An Introduction, Third Revised and Enlarged Edition*, Springer, Berlin, Germany, 1999, pp.293-299.

[13] J. Chen, J. Liu, et al., "Multi-angular optical remote sensing for assessing vegetation structure and carbon absorption, *Remote Sensing of Environment*, 2003, 84(4): pp.516-525

[14] A. Lotsch, Y. Tian, et al., Land cover mapping in support of LAI and FPAR retrievals from EOS-MODIS and MISR: classification methods and sensitivities to errors, *International Journal of Remote Sensing*, 2003, 24 (10): pp.1997-2016

[15] F. J. Tapiador and J. L. Casanova, "An algorithm for the fusion of images based on Jaynes' maximum entropy method." *International Journal of Remote Sensing*, 2002, 23(4):pp.777-785